mathematics

MDPI

Article

Analysis Time-Delayed SEIR Model with Survival Rate for COVID-19 Stability and Disease Control

M. H. Hassan [1,2,*], Tamer El-Azab [2], Ghada AlNemer [3], M. A. Sohaly [2] and H. El-Metwally [2]

[1] October High Institute for Engineering and Technology, Giza 12596, Egypt
[2] Department of Mathematics, Faculty of Science, Mansoura University, Mansoura 35516, Egypt; dr_tamerazab@yahoo.com (T.E.-A.); m_abdelrahman@mans.edu.eg (M.A.S.); eaash69@yahoo.com (H.E.-M.)
[3] Department of Mathematical Sciences, College of Sciences, Princess Nourah bint Abdulrahman University, Riyadh 11671, Saudi Arabia; gnnemer@pnu.edu.sa
* Correspondence: mohamed.hassan445@yahoo.com

Abstract: This paper presents a mathematical model to examine the transmission and stability dynamics of the SEIR model for COVID-19. To assess disease progression, the model incorporates a time delay for the time delay and survival rates. Then, we use the Routh–Hurwitz criterion, the LaSalle stability principle, and Hopf bifurcation analysis to look at disease-free and endemic equilibrium points. We investigate global stability using the Lyapunov function and simulate the model behavior with real COVID-19 data from Indonesia. The results confirm the impact of time delay on disease transmission, mitigation strategies, and population recovery rates, demonstrating that rapid interventions can significantly impact the course of the epidemic. The results indicate that a balance between transmission reduction and vaccination efforts is crucial for achieving long-term stability and controlling disease outbreaks. Finally, we estimate the degree of disease control and look at the rate of disease spread by simulating the genuine data.

Keywords: SEIR model; delay differential equations; stability analysis; Hopf bifurcation; Lyapunov function; COVID-19

MSC: 40D05; 40D25; 42C10; 43A55; 46A35; 46B15

Citation: Hassan, M.H.; El-Azab, T.; AlNemer, G.; Sohaly, M.A.; El-Metwally, H. Analysis Time-Delayed SEIR Model with Survival Rate for COVID-19 Stability and Disease Control. *Mathematics* **2024**, *12*, 3697. https://doi.org/10.3390/math12233697

Academic Editor: Necibe Tuncer

Received: 19 October 2024
Revised: 18 November 2024
Accepted: 20 November 2024
Published: 26 November 2024

1. Introduction

Diseases and infections have always presented an imminent threat to both people and animals. Diseases transmitted by blood or physical touch are known as communicable diseases. Infections and diseases can also be transmitted by inhaling an airborne virus or being bitten by a virus carrier. Moreover, breathing in airborne viruses or being attacked by virus carriers can spread infections and diseases. These diseases and infections have the potential to spread widely, resulting in pain, losses to the community, and financial damages. These diseases cost millions of lives each year, especially in developing countries. Mathematical modeling is an excellent tool for studying these diseases from various perspectives, estimating potential losses, and developing strategies to combat them. Utilizing mathematical modeling to investigate these diseases from many perspectives, predict possible losses, and create strategies is a great idea. We followed these references [1–9] since numerous models have been created to investigate the rates of transmission of various endemic species.

Many authors have investigated epidemiological models with latent or incubation periods because several diseases, like tuberculosis and influenza, have a period in which an individual is diseased but not yet infectious. A typical technique to illustrate this incubation period is to introduce an exposed class [10] or apply a delay effect [11]. As a result, it is vital to compare these two modeling strategies with the incubation time.

All SIR, SIS, SIRS, and SEIR epidemic models utilize delay differential equations (DDEs) to simulate different infectious durations. Hethcote and van den Driessche [12] analyzed an SIS epidemic model that considers the length of infectiousness and has a constant time delay. Global stability in a SIR epidemic model with a given delay, which characterizes the time it takes for an individual to lose infectiousness, was analyzed by Beretta et al. [13]. Song and Cheng [14] investigated how time delay affects the stability of an endemic equilibrium.

Plenty of authors have investigated the global stability of SIR, SIRS, SIS, and SEIR models extensively, employing the directed Lyapunov technique to establish it. The development of a Lyapunov function has made it easier to study global stability at the endemic equilibrium point. We studied the following references to learn more about the Lyapunov function [15–18]. For instance, the SEIR model is one of the models used to study infectious diseases, where S stands for susceptible, a healthy person who is susceptible to infection; E for exposed, a person infected with the disease but not yet contagious, meaning the disease is in its incubation period; I for infectious, a person who can infect others before showing symptoms; and R for recovered, a person who has recovered from the disease due to vaccination or isolation. For more details related to epidemic models and infectious diseases like the SEIR model, we refer to these references [12,13,19].

In epidemiology, Hopf bifurcation is a crucial dynamic phenomenon. It can be used to interpret the periodic behavior of different infectious diseases. We refer the reader to [20–26] for more details about a Hopf bifurcation. It has been shown that delays can affect a system's dynamic behavior in a complex way.

Suwardi Annas, etc. in [27] analyzed the stability of the COVID-19 pandemic's transmission throughout Indonesia and presented the SEIR model as the model Equation (1):

$$\begin{aligned}
\frac{dS(t)}{dt} &= \kappa - (\eta I(t) + \kappa + \vartheta)S(t),\\
\frac{dE(t)}{dt} &= \eta I(t)S(t) - (\theta + \kappa)E(t),\\
\frac{dI(t)}{dt} &= \theta E(t) - (\epsilon + \sigma + \kappa)I(t),\\
\frac{dR(t)}{dt} &= \sigma I(t) + \vartheta S(t) - \kappa R(t),
\end{aligned} \tag{1}$$

where $N(t) = S(t) + E(t) + I(t) + R(t)$ represents the human population, S represents the number of susceptible individuals, E represents the number of exposed individuals, I represents the number of infected individuals, R represents the number of recovered individuals, with κ the rate of birth or death population, η is the probability of changing from S to E, θ is the probability of changing from E to I, with the rate of death population by COVID-19, ϵ, σ is the probability of changing from I to R, and ϑ is the vaccine of the susceptible population.

Many diseases' incubation periods are well-established. For example, it takes three to fourteen days for dengue fever symptoms to manifest, seven days for the bird flu latent period to manifest, and up to a year or more for the rabies incubation period to last. As a result, there is a connection between the current disease spread and a certain past quantity that can be easily observed as a constant number.

Applying the SEIR mathematical model, a research project was performed to investigate the spread of COVID-19. The model was built using the SEIR model, which is presented in [28]. The generation matrix approach, as detailed in [29], was utilized in the model analysis to determine the basic reproduction number and general stability of COVID-19 propagation. We obtained secondary data on COVID-19 in Indonesia from [30] to conduct computational simulations of the model, and then simulated our results to estimate and mitigate the number of COVID-19 cases in Indonesia.

To the best of our knowledge, there is no previous literature specifically dealing with model Equation (1) in the case of time delay that represents the improvement of the results

in [27]. Therefore, our motivation in this paper is to provide the modification of the model Equation (1) by adding the time delay, ξ, for S, I comparables, knowing that the fraction of infected individuals and the survival rate is the $e^{-\kappa\xi}$ term at time t. We then go on to discuss the Hopf bifurcation and stability analysis of the SEIR model, which is represented in the model Equation (2). Finally, we rate this model by numerically simulating some data. The following is the structure of the model Equation (2):

$$\begin{aligned}
\frac{dS(t)}{dt} &= \kappa - \eta I(t-\xi)S(t-\xi)e^{-\kappa\xi} - (\kappa+\vartheta)S(t),\\
\frac{dE(t)}{dt} &= \eta I(t-\xi)S(t-\xi)e^{-\kappa\xi} - (\theta+\kappa)E(t),\\
\frac{dI(t)}{dt} &= \theta E(t) - (\epsilon+\sigma+\kappa)I(t),\\
\frac{dR(t)}{dt} &= \sigma I(t) + \vartheta S(t) - \kappa R(t).
\end{aligned} \tag{2}$$

On the other hand, $\xi > 0$ refers to the time before exposure to injury as a result of a decrease in social interaction, either as a result of government-implemented disease control measures or as a voluntary choice made by citizens.

This work aims to explore the analysis of local stability in both endemic and disease-free equilibriums. After that, we use the Lyapunov function to investigate the epidemic equilibrium's global stability. Thus, we use the delay, ξ, as a parameter to examine the Hopf bifurcation and show that a Hopf bifurcation occurs when the positive equilibrium loses stability due to a delay that exceeds a threshold value. Finally, we employ a simulation of the actual data to determine the degree of strength, moderateness, or weakness of disease control and to look at the rate of disease transmission.

The organization of this paper is as follows. In Section 2, we recognize the existence of positive equilibrium and examine the local stability in the equilibriums, including both the epidemic and disease-free states. After that, we use the global stability of Lyapunov function equilibrium to investigate the endemic situation. In Section 3, we use the linearized system's characteristic Equation (2) to determine whether Hopf bifurcations exist at the epidemic equilibrium point. In Section 4, we use the Maple tool to determine the equilibrium points, find the next generation matrix, and find the Jacobian to determine the eigenvalues, and then use Matlab to simulate data to illustrate the level of disease control and the disease's rate of spread using the dde23 function.

2. The Stability Analysis of Equilibria

This section examines both the model equation's endemic equilibrium Equation (2) and the local stability of a disease-free equilibrium.

2.1. Some Results and Discussion

In this part of the article, our focus is on the disease-free and endemic equilibrium points. These points are given by

(i) The first point is a disease-free equilibrium where there is no spread of disease and that satisfies the conditions $E = I = 0$. It is given by

$$E_0 = (S, E, I, R) = \left(\frac{\kappa}{\kappa+\vartheta}, 0, 0, \frac{\vartheta}{(\kappa+\vartheta)}\right). \tag{3}$$

(ii) The second point is endemic equilibrium that is used to predict the spread of disease and satisfy the conditions $S \neq 0$, $E \neq 0$, $I \neq 0$, and $R \neq 0$. So that

$$E_1 = (S, E, I, R) = \begin{pmatrix} \frac{(\epsilon+\sigma+\kappa)(\kappa+\theta)}{\eta\theta e^{-\kappa\xi}}, \\ \frac{\eta\kappa\theta e^{-\kappa\xi} - (\epsilon+\sigma+\kappa)(\kappa+\theta)(\kappa+\vartheta)}{\eta\theta(\kappa+\theta)e^{\kappa\xi}}, \\ \frac{\eta\theta\kappa e^{-\kappa\xi} - (\epsilon+\sigma+\kappa)(\kappa+\theta)(\kappa+\vartheta)}{\eta(\epsilon+\sigma+\kappa)(\kappa+\theta)e^{-\kappa\xi}}, \\ \frac{\eta\theta^2\sigma\kappa e^{-\kappa\xi} + (\epsilon+\sigma+\kappa)(\kappa+\theta)[\kappa^2\vartheta + ((\vartheta-\sigma)\theta + \vartheta(\sigma+\epsilon))\kappa + \vartheta\theta\epsilon]}{\eta(\epsilon+\sigma+\kappa)(\kappa+\theta)\theta\kappa e^{\kappa\xi}}. \end{pmatrix} \quad (4)$$

The Basic Number of Reproduction $\Re_0$

The expected value of multiple vulnerable populations contracting the infection during the endemic is represented by the basic reproduction number. Equations containing only infection can be used to calculate basic reproduction numbers. The approach used to calculate basic reproduction numbers employs the next-generation matrix G, which is defined as:

$$G = \mathcal{F}V^{-1}.$$

The first step to find G, we obtain

$$F_1 = \begin{bmatrix} \eta ISe^{-\kappa\xi} \\ 0 \end{bmatrix}, \; V_1 = \begin{bmatrix} (\theta+\kappa)E \\ \theta E - (\epsilon+\sigma+\kappa)I \end{bmatrix}.$$

Then we obtain $\mathcal{F}$ and V^{-1} matrices as follows:

$$\mathcal{F} = \begin{pmatrix} 0 & \eta Se^{-\kappa\xi} \\ 0 & 0 \end{pmatrix}, V^{-1} = \begin{pmatrix} \frac{1}{(\theta+\kappa)} & 0 \\ \frac{\theta}{(\theta+\kappa)(\epsilon+\sigma+\kappa)} & \frac{-1}{(\epsilon+\sigma+\kappa)} \end{pmatrix}.$$

And then by substituting E_0, we obtain

$$\Re_0 = \frac{\eta\kappa e^{-\kappa\xi}\theta}{(\theta+\kappa)(\epsilon+\sigma+\kappa)(\kappa+\vartheta)}.$$

So that the endemic equilibrium point, E_1, can be written as:

$$E_1 = (S, E, I, R) = \begin{pmatrix} \frac{\kappa}{(\kappa+\vartheta)\Re_0}, \\ \frac{\kappa}{(\kappa+\theta)}(1 - \frac{1}{\Re_0}), \\ \frac{(\kappa+\vartheta)}{\eta e^{-\kappa\xi}}(\Re_0 - 1), \\ \frac{\sigma(\kappa+\vartheta)^2(\epsilon+\sigma+\kappa)(\kappa+\theta)\Re_0 + \eta\kappa e^{-\kappa\xi}[\kappa^2\vartheta + ((\vartheta-\sigma)\theta + \vartheta(\sigma+\epsilon))\kappa + \vartheta\theta\epsilon]}{\eta\kappa(\epsilon+\sigma+\kappa)(\kappa+\theta)(\kappa+\vartheta)e^{-\kappa\xi}\Re_0}. \end{pmatrix}$$

2.2. The Analysis of Local Stability

This part discusses the local stability of the endemic, E_1, and the disease-free equilibrium, E_0. We obtained the Jacobian matrices of the proposed SEIR model with a model Equation (2) as follows:

$$J = \begin{pmatrix} -\eta Ie^{-\kappa\xi}e^{-\varrho\xi} - \kappa - \vartheta & 0 & -\eta Se^{-\kappa\xi}e^{-\varrho\xi} & 0 \\ \eta Ie^{-\kappa\xi}e^{-\varrho\xi} & -\kappa-\theta & \eta Se^{-\kappa\xi}e^{-\varrho\xi} & 0 \\ 0 & \theta & -\epsilon-\sigma-\kappa & 0 \\ \vartheta & 0 & \sigma & -\kappa \end{pmatrix}. \quad (5)$$

Consequently, we have to determine the Jacobian matrix's eigenvalue in Equation (5) by

$$\det(J-\varrho I)=\begin{vmatrix} -\eta I e^{-\kappa\xi}e^{-\varrho\xi}-\kappa-\vartheta-\varrho & 0 & -\eta S e^{-\kappa\xi}e^{-\varrho\xi} & 0 \\ \eta I e^{-\kappa\xi}e^{-\varrho\xi} & -\kappa-\theta-\varrho & \eta S e^{-\kappa\xi}e^{-\varrho\xi} & 0 \\ 0 & \theta & -\epsilon-\sigma-\kappa-\varrho & 0 \\ \vartheta & 0 & \sigma & -\kappa-\varrho \end{vmatrix}=0.$$

Now, in the following theorem, we discuss the stability of the first equilibrium point, E_0, if $\Re_0<1$, for all $\xi\geq 0$.

Theorem 1. *The equilibrium free of disease if* $\Re_0<1$, *then* E_0 *is locally asymptotically stable; otherwise,* E_0 *is unstable for all* $\xi\geq 0$.

Proof. Using $\det(J-\varrho I)_{E_0}=0$, we can obtain the characteristic equation of E_0:

$$(\kappa+\varrho)(\kappa+\vartheta+\varrho)\left[(\epsilon+\sigma+\kappa+\varrho)(\kappa+\theta+\varrho)-\frac{\eta\theta\kappa e^{-\kappa\xi}e^{-\varrho\xi}}{(\kappa+\vartheta)}\right]=0. \tag{6}$$

So that

$$(\kappa+\varrho)(\kappa+\vartheta+\varrho)\left[\varrho^2+\varrho(2\kappa+\theta+\epsilon+\sigma)+(\epsilon+\sigma+\kappa)(\kappa+\theta)-\frac{\eta\theta\kappa e^{-\kappa\xi}e^{-\varrho\xi}}{(\kappa+\vartheta)}\right]=0. \tag{7}$$

Then from Equation (6), the eigenvalues evaluated at E_0 are $\varrho_1=-(\kappa+\vartheta)<0$, $\varrho_2=-\kappa<0$, we have

$$\varrho^2+\varrho(2\kappa+\theta+\epsilon+\sigma)+(\epsilon+\sigma+\kappa)(\kappa+\theta)-\frac{\eta\theta\kappa e^{-\kappa\xi}e^{-\varrho\xi}}{(\kappa+\vartheta)}=0. \tag{8}$$

For $\xi=0$, Equation (8) becomes

$$\varrho^2+\varrho(2\kappa+\theta+\epsilon+\sigma)+(\epsilon+\sigma+\kappa)(\kappa+\theta)(1-\Re_0)=0. \tag{9}$$

Thus, the roots of Equation (9) contain negative real parts if $\Re_0<1$. Therefore, E_0 is unstable by the Routh criteria if $\Re_0>1$.

For $\xi>0$, let $\varrho=i\varpi$, where $\varpi>0$. Substituting $\varrho=i\varpi$ into Equation (8), we obtain

$$-\varpi^2+i(2\kappa+\theta+\epsilon+\sigma)\varpi+(\epsilon+\sigma+\kappa)(\kappa+\theta)-\frac{\eta\theta\kappa e^{-\kappa\xi}}{(\kappa+\vartheta)}(\cos\varpi\xi-i\sin\varpi\xi)=0. \tag{10}$$

Hence, we obtain the real and imaginary parts, as

$$\begin{aligned} \frac{\eta\theta\kappa e^{-\kappa\xi}}{(\kappa+\vartheta)}\cos\varpi\xi&=(\epsilon+\sigma+\kappa)(\kappa+\theta)-\varpi^2, \\ \frac{\eta\theta\kappa e^{-\kappa\xi}}{(\kappa+\vartheta)}\sin\varpi\xi&=-\varpi(2\kappa+\theta+\epsilon+\sigma). \end{aligned} \tag{11}$$

After the two equations in (11) are squared and added, this produces

$$\varpi^4+\left[(\epsilon+\sigma+\kappa)^2+(\kappa+\theta)^2\right]\varpi^2+(\epsilon+\sigma+\kappa)^2(\kappa+\theta)^2-\frac{\eta^2\theta^2\kappa^2e^{-2\kappa\xi}}{(\kappa+\vartheta)^2}=0. \tag{12}$$

The Equation (12) can be written as

$$\varpi^4+\left[(\epsilon+\sigma+\kappa)^2+(\kappa+\theta)^2\right]\varpi^2+(\epsilon+\sigma+\kappa)^2(\kappa+\theta)^2(1-\Re_0^2)=0. \tag{13}$$

Let $Q = \varpi^2$, also we denote

$$a = \left[(\epsilon + \sigma + \kappa)^2 + (\kappa + \theta)^2\right], b = (\epsilon + \sigma + \kappa)^2(\kappa + \theta)^2(1 - \Re_0^2).$$

After that Equation (13) can be written as

$$Q^2 + aQ + b = 0.$$

For Equation (13), it is evident that the roots have negative real parts if $\Re_0 < 1$. If $\xi \neq 0$, then E_0 is not locally asymptotically stable. Ruan and Wei state that E_0 is unstable if $\Re_0 > 1$ (see [31] [Corollary 2.4]). □

At this point, assuming $\Re_0 > 1$ for $\xi \geq 0$, we concentrate on the local stability of the endemic equilibrium point, E_1.

Theorem 2. *The equilibrium of endemic if $\Re_0 > 1$, then E_1 is locally asymptotically stable; otherwise, E_1 is unstable for all $\xi \geq 0$.*

Proof. The characteristic of Equation (5) evaluated at E_1 is a fourth-degree polynomial as follows

$$\varrho^4 + \hbar_1\varrho^3 + \hbar_2\varrho^2 + \hbar_3\varrho + \hbar_4 + \left(l_1\varrho^3 + l_2\varrho^2 + l_3\varrho + l_4\right)e^{-\varrho\xi} = 0, \tag{14}$$

whereas

$$\begin{aligned}
\hbar_1 &= 4\kappa + \sigma + \epsilon + \theta + \vartheta,\\
\hbar_2 &= (\epsilon + \sigma + \kappa)(\kappa + \theta) + (\kappa + \vartheta) + \kappa(3\kappa + \vartheta + \sigma + \epsilon + \theta),\\
\hbar_3 &= (\epsilon + \sigma + \kappa)(\kappa + \theta)(\kappa + \vartheta) + \kappa[(\kappa + \vartheta) + (\epsilon + \sigma + \kappa)(\kappa + \theta)],\\
\hbar_4 &= \kappa(\epsilon + \sigma + \kappa)(\kappa + \theta)(\kappa + \vartheta)\\
l_1 &= (\kappa + \vartheta)(\Re_0 - 1),\\
l_2 &= (\kappa + \vartheta)(2\kappa + \sigma + \epsilon)(\Re_0 - 1) - \frac{\eta\theta\kappa e^{-\kappa\xi}}{(\kappa + \vartheta)\Re_0} + \kappa(\kappa + \vartheta)(\Re_0 - 1),\\
l_3 &= [(\epsilon + \sigma + \kappa)(\kappa + \theta) + \kappa(2\kappa + \sigma + \epsilon + \theta)](\kappa + \vartheta)(\Re_0 - 1) - \frac{\eta\theta\kappa e^{-\kappa\xi}}{\Re_0}\left[1 + \frac{\kappa}{(\kappa + \vartheta)}\right],\\
l_4 &= \kappa(\epsilon + \sigma + \kappa)(\kappa + \theta)(\kappa + \vartheta)(\Re_0 - 1) - \frac{\eta\theta\kappa^2 e^{-\kappa\xi}}{\Re_0}.
\end{aligned}$$

For $\xi = 0$, Equation (14) becomes

$$\varrho^4 + a_1\varrho^3 + a_2\varrho^2 + a_3\varrho + a_4 = 0, \tag{15}$$

where

$$\begin{aligned}
a_0 &= 1,\\
a_1 &= \hbar_1 + l_1 = (4\kappa + \sigma + \epsilon + \theta + \vartheta) + (\kappa + \vartheta)(\Re_0 - 1),\\
a_2 &= \hbar_2 + l_2 = [(\epsilon + \sigma + \kappa)(\kappa + \theta) + (\kappa + \vartheta) + \kappa(3\kappa + \vartheta + \sigma + \epsilon + \theta)]\\
&\quad + (\kappa + \vartheta)(\Re_0 - 1)(3\kappa + \sigma + \epsilon) - \frac{\eta\theta\kappa e^{-\kappa\xi}}{(\kappa + \vartheta)\Re_0},\\
a_3 &= \hbar_3 + l_3 = (\epsilon + \sigma + \kappa)(\kappa + \theta)(\kappa + \vartheta) + \kappa[(\kappa + \vartheta) + (\epsilon + \sigma + \kappa)(\kappa + \theta)]\\
&\quad + [(\epsilon + \sigma + \kappa)(\kappa + \theta) + \kappa(2\kappa + \sigma + \epsilon + \theta)](\kappa + \vartheta)(\Re_0 - 1) - \frac{\eta\theta\kappa e^{-\kappa\xi}}{\Re_0}\left[1 + \frac{\kappa}{(\kappa + \vartheta)}\right],\\
a_4 &= \hbar_4 + l_4 = \kappa(\kappa + \vartheta)(\epsilon + \sigma + \kappa)(\kappa + \theta)\Re_0 - \frac{\eta\theta\kappa^2 e^{-\kappa\xi}}{\Re_0}.
\end{aligned}$$

If $\Re_0 > 1$, it is evident that $a_i > 0$, where $i = 0, 1, 2, 3$, thereby

$$\left.\begin{array}{c} a_0, a_1 > 0, a_1a_2 - a_3 > 0, \\ a_3(a_1a_2 - a_3) - a_4a_1^2 > 0, a_4 > 0. \end{array}\right\} \tag{16}$$

Then, according to the Routh–Hurwitz criterion, all distinctive roots of Equation (16) have negative real parts [32]. Therefore, E_1 is locally asymptotically stable.

When $\xi > 0$, we assume $\varpi > 0$ and $\varrho = \varpi i$. Consequently, by modifying Equation (14) to have $\varrho = \varpi i$, we find

$$\varpi^4 - i\hbar_1\varpi^3 - \hbar_2\varpi^2 + i\varpi\hbar_3 + \hbar_4 + (-i\varpi^3 l_1 - \varpi^2 l_2 + i\varpi l_3 + l_4)(\cos\varpi\xi - i\sin\varpi\xi) = 0.$$

After the separation of the real and imaginary parts, the result is

$$\left.\begin{array}{c} (l_2\varpi^2 - l_4)\cos\varpi\xi + (l_1\varpi^3 - l_3\varpi)\sin\varpi\xi = \varpi^4 - \hbar_2\varpi^2 + \hbar_4, \\ (l_1\varpi^3 - l_3\varpi)\cos\varpi\xi - (\varpi^2 l_2 - l_4)\sin\varpi\xi = \hbar_3\varpi - \hbar_1\varpi^3. \end{array}\right\} \tag{17}$$

Squaring and adding both equations gives

$$\left.\begin{array}{c} \varpi^8 + (\hbar_1^2 - 2\hbar_2 - l_1^2)\varpi^6 + (\hbar_2^2 - 2\hbar_1\hbar_3 - l_2^2 + 2l_1l_3 + 2\hbar_4)\varpi^4 + \\ +(\hbar_3^2 + 2l_2l_4 - 2\hbar_2\hbar_4 - l_3^2)\varpi^2 + \hbar_4^2 - l_4^2 = 0. \end{array}\right\} \tag{18}$$

Assuming that $Q = \varpi^2$, then Equation (18) can be written in the form

$$Q^4 + \hbar Q^3 + lQ^2 + mQ + n = 0, \tag{19}$$

where

$$\left.\begin{array}{c} \hbar = \hbar_1^2 - 2\hbar_2 - l_1^2, \\ l = \hbar_2^2 - 2\hbar_1\hbar_3 - l_2^2 + 2l_1l_3 + 2\hbar_4, \\ m = \hbar_3^2 + 2l_2l_4 - 2\hbar_2\hbar_4 - l_3^2, \\ n = \hbar_4^2 - l_4^2. \end{array}\right\} \tag{20}$$

Lemma 3.3.1 in [33] is satisfied if $\Re_0 > 1$, $\hbar, l, m, n$ given in Equation (20), respectively, are positive. □

Lemma 1. *Equation (19) has no positive real roots if* $\hbar \geq 0$, $m \geq 0$, $l > 0$, *and* $n > 0$.

Proof. The left side of Equation (19) is known as

$$f(Q) = Q^4 + \hbar Q^3 + lQ^2 + mQ + n. \tag{21}$$

The derivative of $f(Q)$ with respect to Q consequently is obtained as follows:

$$f^{'}(Q) = 4Q^3 + 3\hbar Q^2 + 2lQ + m. \tag{22}$$

Knowing that $f^{'}(Q) > 0$ for $Q \geq 0$ indicates that the function $f(Q)$ is increasing for $Q \geq 0$. Equation (19) has no positive real roots since $f(0) = n \geq 0$. □

Remark 1. *There is no* ϖ *such that* $i\varpi$ *is an eigenvalue of characteristic Equation (19), according to Lemma 1. Consequently, for all values of the delay* $\xi \geq 0$, *the real part of all eigenvalues of Equation (15) is negative according to Rouché's theorem [34] ([Theorem 9.17.4]).*

Now we have established the analysis above, we can deduce the following.

Theorem 3. *Suppose that*

(i) $\Re_0 > 1$;
(ii) $\hbar \geq 0, m \geq 0, l > 0$, *and* $n > 0$.

Thus, the endemic equilibrium, E_1, *is stable, and it is locally asymptotically stable for all* ξ *values greater than zero.*

Remark 2. *Theorem 3 states that* E_1 *is locally asymptotically stable for all values of delay* $\xi \geq 0$ *if the parameters satisfy conditions* (i) *and* (ii)*; in contrast,* E_1 *is locally asymptotically stable independent of the delay. The stability of* E_1*, however, depends on the delay value; if the conditions in Theorem 3, in particular, any of the inequalities in* (ii)*, are not satisfied, the endemic equilibrium may lose stability as the delay varies, which could result in oscillations.*

Remark 3. *If* $m < 0$, *then* $\lim_{Q \longrightarrow \infty} f(Q) = \infty$ *and* $f(0) = n < 0$ *are true. For this purpose, Equation (19) has at least one positive root,* Q_1*. As a result,* $\varpi = \sqrt{Q_1}$ *indicates that Equation (18) has at least one positive root.*

2.3. Global Stability of Endemic

In this part, we use Lyapunov's function to study the global stability of the endemic equilibrium point, E_1, of a model Equation (2) if $\Re_0 > 1$.

Theorem 4. ***(Lyapunov Stability Theorem)*** *Assuming that* $\Re_0 > 1$, *the endemic equilibrium point,* E_1, *is globally stable. However, if* $\Re_0 < 1$, *then* E_1 *is unstable.*

Proof. We consider the proposed SEIR model on the first three variables only (S, E, and I). The Lyapunov function on $\mathbb{R}^3_+$ can be represented as follows:

$$V(S,E,I) = \frac{(S-S^*)^2}{2} + \frac{(E-E^*)^2}{2} + \frac{(I-I^*)^2}{2} + \frac{(R-R^*)^2}{2},$$

since $E_1 = (S,E,I) = \left(\frac{\kappa}{(\kappa+\vartheta)\Re_0}, \frac{\kappa}{(\kappa+\theta)}(1-\frac{1}{\Re_0}), \frac{(\kappa+\vartheta)}{\eta e^{-\kappa\xi}}(\Re_0 - 1)\right)$.

It is not difficult to realize that at $S = S^*, E = E^*$, and $I = I^*, R = R^*, V(S,E,I) > 0$ and $V(S,E,I) = 0$. Now, since we have evaluated $V^{'}$s derivative about t, we have

$$V^{'}(S,E,I) = (S-S^*)\frac{dS}{dt} + (E-E^*)\frac{dE}{dt} + (I-I^*)\frac{dI}{dt} + (R-R^*)\frac{dR}{dt}$$

$$= (S-S^*)\left[\kappa - \eta SI\exp^{-\kappa\xi} - (\kappa+\vartheta)S\right] + (E-E^*)\left[\eta SI\exp^{-\kappa\xi} - (\theta+\kappa)E\right]$$
$$+ (I-I^*)[\theta E - (\kappa_1+\sigma+\kappa)I] + (R-R^*)[\sigma I(t) + \vartheta S(t) - \kappa R(t)]$$
$$= -\kappa\left[(S-S^*)\left(\tfrac{\kappa+\vartheta}{\kappa} - 1\right) + (E-E^*)\left(\tfrac{\theta+\kappa}{\kappa}\right)E + (I-I^*)\left(\tfrac{\epsilon+\sigma+\kappa}{\kappa}\right)I\right]$$
$$-\kappa\left[(I-I^*)\left(\tfrac{\theta}{\kappa}\right)E + (R-R^*)\left(\tfrac{\sigma}{\kappa}I(t) + \tfrac{\vartheta}{\kappa}S(t) - R(t)\right)\right]$$
$$-\eta SI\exp^{-\kappa\xi}[(S-S^*) - (E-E^*)]$$
$$= -\kappa\left[(S-S^*)\left(\tfrac{\kappa+\vartheta}{\kappa} - 1\right) + (E-E^*)\left(\tfrac{\theta}{\kappa} + 1\right)E + (I-I^*)\left(\tfrac{\epsilon+\sigma}{\kappa} + 1\right)I\right]$$
$$-\kappa\left[(I-I^*)\left(\tfrac{\theta}{\kappa}\right)E + (R-R^*)\left[\tfrac{\sigma}{\kappa}I(t) + \tfrac{\vartheta}{\kappa}S(t) - R(t)\right]\right]$$
$$-\eta SI\exp^{-\kappa\xi}[(S-S^*) - (E-E^*)] \leq 0.$$

If the following conditions hold:

(a) $S > S^*$ and $\frac{\kappa+\vartheta}{\kappa} - 1 > 0$, then $\frac{\kappa+\vartheta}{\kappa} > 1$.
(b) $E > E^*$ and $\frac{\theta+\kappa}{\kappa} > 0$, then $\frac{\theta}{\kappa} + 1 > 0$ and $\frac{\theta}{\kappa} > -1$.
(c) $I > I^*$ and $\frac{\epsilon+\sigma+\kappa}{\kappa} > 0$, then $\frac{\epsilon+\sigma}{\kappa} + 1 > 0$ and $\frac{\epsilon+\sigma}{\kappa} > -1$.
(d) $V^{'}(S^*,E^*,I^*) = 0$ if $S = S^*, E = E^*$, and $I = I^*$.

Thus, the model Equation (2) is globally stable at E_1 with $\Re_0 > 1$ if it satisfies the conditions (a)–(d). □

3. Analysis of Hopf Bifurcation

In this section, we use the time delay, ξ, as the bifurcation parameter to illustrate and find the conditions in which Hopf bifurcation occurs. The endemic equilibrium, E_1, and the condition $\Re_0 > 1$ are assumed throughout this section.

We now turn to the analysis of bifurcations. As functions of the bifurcation parameter ξ, we present the solutions of Equation (15).

Theorem 5. *Given that ϖ_1 is the largest positive simple of Equation (18) and*

(i) $m < 0$ *or*
(ii) $m \geq 0$ *and* $n < 0$

are satisfied, let us assume that $\Re_0 > 1$. In this case, E_1 is asymptotically unstable when $\xi > \xi_1$ and stable when $\xi < \xi_1$, where

$$\xi_1 = \frac{1}{\varpi_1} \arccos\left[\frac{(l_2\varpi_1^2 - l_4)(\varpi_1^4 - \hbar_2\varpi + \hbar_4) + (l_1\varpi_1^3 - l_3\varpi)(\hbar_3\varpi_1 - \hbar_1\varpi_1^3)}{(l_2\varpi_1^2 - l_4)^2 + (l_1\varpi_1^3 - l_3\varpi)^2}\right].$$

The Hopf bifurcation, where ξ passes through the critical value ξ_1, is a family of periodic solutions that bifurcates from E_1 when $\xi = \xi_1$.

Proof. Let $\varrho(\xi) = \kappa(\xi) + i\varpi(\xi)$ be the eigenvalues of Equation (14), such that $\kappa(\xi_1) = 0$ and $\varpi(\xi_1) = \varpi_1$ for a given initial value of the bifurcation parameter ξ_1.

Assuming that $\varpi_1 > 0$, we can deduce the following from Equation (17)

$$\left.\begin{aligned}(l_2\varpi^2 - l_4)\cos\varpi\xi + (l_1\varpi^3 - l_3\varpi)\sin\varpi\xi &= \varpi^4 - \hbar_2\varpi^2 + \hbar_4,\\ (l_1\varpi^3 - l_3\varpi)\cos\varpi\xi - (\varpi^2 l_2 - l_4)\sin\varpi\xi &= \hbar_3\varpi - \hbar_1\varpi^3.\end{aligned}\right\}$$

So, we obtain that

$$\xi_1 = \frac{1}{\varpi_1} \arccos\left[\frac{(l_2\varpi_1^2 - l_4)(\varpi_1^4 - \hbar_2\varpi + \hbar_4) + (l_1\varpi_1^3 - l_3\varpi)(\hbar_3\varpi_1 - \hbar_1\varpi_1^3)}{(l_2\varpi_1^2 - l_4)^2 + (l_1\varpi_1^3 - l_3\varpi)^2}\right] + \frac{2j\pi}{\varpi_1}, \quad j = 0, 1, 2, \ldots$$

We can additionally confirm the subsequent transversal condition

$$\left.\frac{d\,\mathrm{Re}\,\varrho(\xi)}{d\xi}\right|_{\xi=\xi_1} > 0.$$

When $\xi > \xi_1$, the steady state becomes unstable, and the real part of $\varrho(\xi)$ becomes positive by continuity. In addition, ξ passes a critical rate ξ_1 at which a Hopf bifurcation occurs; we refer to [20,33]. By differentiating Equation (14) in regards to ξ, we find

$$\left.\begin{aligned}[4\varrho^3 + 3\hbar_1\varrho^2 + 2\hbar_2\varrho + \hbar_3 + [3l_1\varrho^2 + 2l_2\varrho + l_4 - \xi(l_1\varrho^3 + l_2\varrho^2 + l_3\varrho + l_4)]e^{-\varrho\xi}]\tfrac{d\varrho}{d\xi}\\ = \varrho e^{-\varrho\xi}(l_1\varrho^3 + l_2\varrho^2 + l_3\varrho + l_4).\end{aligned}\right\}$$

Then

$$\left(\frac{d\varrho}{d\xi}\right)^{-1} = \frac{4\varrho^3 + 3\hbar_1\varrho^2 + 2\hbar_2\varrho + \hbar_3 + (3l_1\varrho^2 + 2l_2\varrho + l_4)e^{\varrho\xi}\xi(l_1\varrho^3 + l_2\varrho^2 + l_3\varrho + l_4)]e^{-\varrho\xi}}{\varrho e^{-\varrho\xi}(l_1\varrho^3 + l_2\varrho^2 + l_3\varrho + l_4)}$$

$$= \frac{4\varrho^3 + 3\hbar_1\varrho^2 + 2\hbar_2\varrho + \hbar_3}{\varrho e^{-\varrho\xi}(l_1\varrho^3 + l_2\varrho^2 + l_3\varrho + l_4)} + \frac{(3l_1\varrho^2 + 2l_2\varrho + l_4)e^{-\varrho\xi}}{\varrho e^{-\varrho\xi}(l_1\varrho^3 + l_2\varrho^2 + l_3\varrho + l_4)} - \frac{\xi}{\varrho}$$

$$= -\frac{(3\varrho^4 + 2\hbar_1\varrho^3 + \hbar_2\varrho^2 - \hbar_4)}{\varrho^2(\varrho^4 + \hbar_1\varrho^3 + \hbar_2\varrho^2 + \hbar_3\varrho + \hbar_4)} + \frac{2l_1\varrho^3 + l_2\varrho^2 - l_4}{\varrho^2(\varrho^4 + l_1\varrho^3 + l_2\varrho^2 + l_3\varrho + l_4)} - \frac{\xi}{\varrho}$$

Therefore,

$$\begin{aligned}
&\operatorname{sign}\left\{\frac{d(\operatorname{Re}\varrho)}{d\xi}\right\}\Big|_{\varrho i\omega_1} = \operatorname{sign}\left\{\operatorname{Re}\left(\frac{d\varrho}{d\xi}\right)^{-1}\right\}\Big|_{\varrho=i\omega_1}\\
&= sign\operatorname{Re}\left[-\frac{(3\varrho^4+2\hbar_1\varrho^3+\hbar_2\varrho^2-\hbar_4)}{\varrho^2(\varrho^4+\hbar_1\varrho^3+\hbar_2\varrho^2+\hbar_3\varrho+\hbar_4)}+\frac{2l_1\varrho^3+l_2\varrho^2-l_4}{\varrho^2(\varrho^4+l_1\varrho^3+l_2\varrho^2+l_3\varrho+l_4)}-\frac{\xi}{\varrho}\right]_{\varrho=i\omega_1}\\
&= sign\left[\frac{(3\omega_1^4-\hbar_2\omega_1^2-\hbar_4)(\omega_1^4-\hbar_2\omega_1^2+\hbar_4)-2\hbar_1\omega_1^3(\hbar_3\omega_1-\hbar_1\omega_1^3)}{\omega_1^2[(\omega_1^4-\hbar_2\omega_1^2+\hbar_4)^2+(\hbar_3\omega_1-\hbar_1\omega_1^3)^2]}\right]\\
&+ sign\left[\frac{(l_3+l_1\omega_1^2)(l_3-l_1\omega_1^2)}{\omega_1^2[(l_4-l_2\omega_1^2)^2+(l_3\omega_1-l_1\omega_1^3)^2]}\right]\\
&= sign\left\{\frac{3\omega_1^8+2(\hbar_1^2-2\hbar_2-l_1^2)\omega_1^6+(2\hbar_4+\hbar_2^2-2\hbar_2\hbar_3+2l_1l_3-l_2^2)\omega_1^4-(\hbar_4^2-l_4^2)}{\omega_1^2[(\omega_1^4-\hbar_2\omega_1^2+\hbar_4)^2+(\hbar_3\omega_1-\hbar_1\omega_1^3)^2]}\right\}\\
&= sign\left\{\frac{3\omega_1^8+2\hbar\omega_1^6+l\omega_1^4-n}{\omega_1^2[(\omega_1^4-\hbar_2\omega_1^2+\hbar_4)^2+(\hbar_3\omega_1-\hbar_1\omega_1^3)^2]}\right\}
\end{aligned}$$

From Equation (21), we obtain

$$f(Q) = Q^4+\hbar Q^3+lQ^2+mQ+n.$$

Here, $\hbar, l > 0$ and $m > 0, n > 0$. As ω_1 is the largest positive simple root of Equation (18), we obtain

$$\frac{d(\operatorname{Re}\varrho)}{d\xi}\Big|_{\omega=\omega_1,\xi=\xi_1} > 0.$$

According to Rouché's theorem [3], the root of characteristic Equation (15) continuously varies from a value less than ξ_1 to one greater than ξ_1, crossing the imaginary axis from the left to the right. As a result, the transversality criterion is satisfied; at $\xi = \xi_1$, the conditions of Hopf bifurcation [35] are satisfied. □

4. Numerical Simulations

In addition to the theoretical analysis of the results in Section 2, we provide some numerical results of the model Equation (2), which includes additional values for ξ, θ, and ϑ to determine if the case of investigation is an epidemic or a free-disease case in this section. Moreover, by analyzing the degree of containment and control as strong, moderate, or weak, we also examine the rate at which the disease is spreading.

The data used in this analysis are real, as shown in Figures 1–4, and we followed these references [36,37]. The initial conditions used to simulate our results are $N = 26960 \times 10^{-2}$, $S_0 = 37358$, $E_0 = 13923$, $I_0 = 23191$, and $R_0 = 13213$. We also depend on some parameters such as $\kappa = 6.25 \times 10^{-3}$, $\eta = 0.62 \times 10^{-8}$, $\sigma = 0.0006667$, and $\epsilon = 7.344 \times 10^{-7}$. The time period here is in days, so for some drawings we used a duration of 60 days, and for others we used a duration of 200 days to clarify the drawings more accurately.

Remark 4. ***Figure 6*** *in [27] indicates more spread, especially with larger β values, and indicating an epidemic state also demonstrates varying levels of control.*

Remark 5. *The worst control is seen in [27]* ***Figure 7****, which indicates a more serious epidemic condition with a marked increase in infected cases before any decrease.*

Remark 6. *Furthermore, in [27], the impact of health measures is seen in* ***Figure 8,*** *which indicates the best control at $\nu = 1\%$, which implies successful measures, and rapid spread at $\nu = 100\%$.*

Remark 7. ***Figure 9*** *in [27] illustrates the highlights of the effectiveness of health measures at low "v" values, leading to high recovery numbers.*

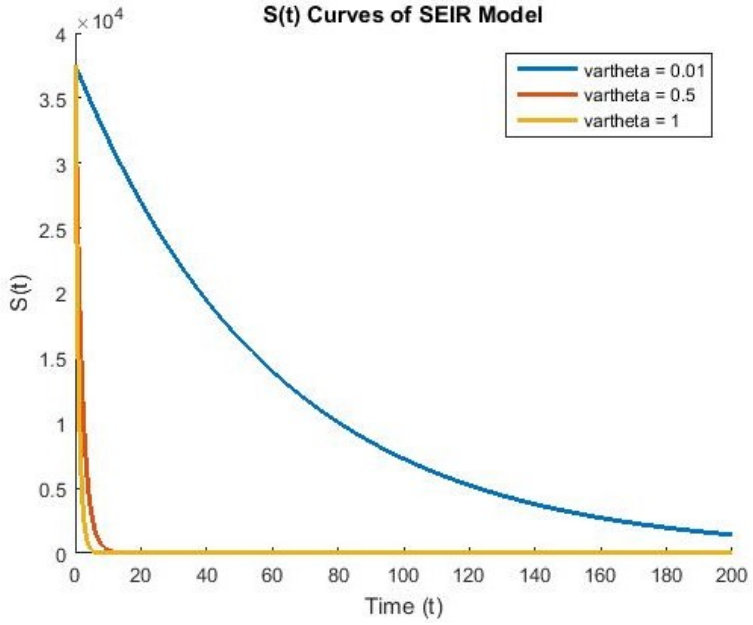

(**a**)

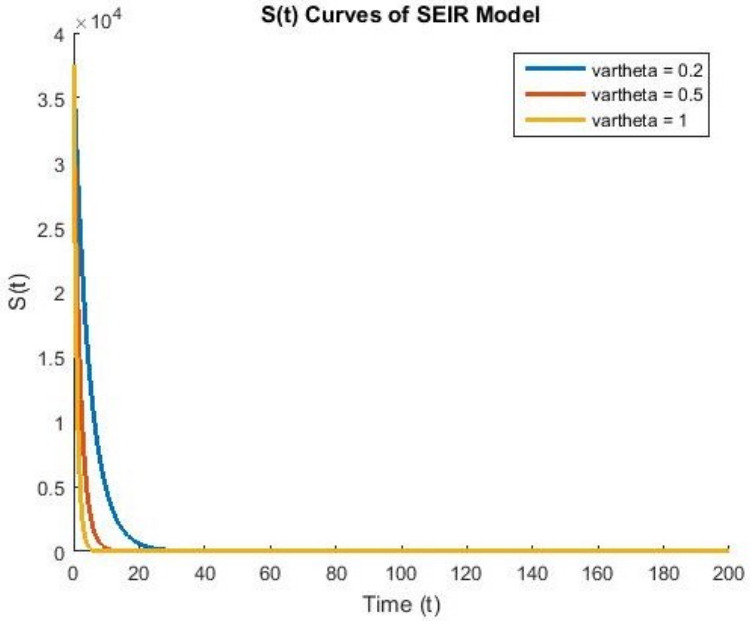

(**b**)

Figure 1. (**a**) in Figure 1 illustrates how values affect the transmission of disease, it is shown that control improves as "ϑ" decreases. In (**b**), $\vartheta = 20\%$ gives the best and excellent control over disease spread, indicating high effectiveness, but $\vartheta = 100\%$ represents the worth control, meaning greater spread. At $\vartheta = 1\%$, the minimal spread represents the best control, and at $\vartheta = 100\%$ the highest spread.

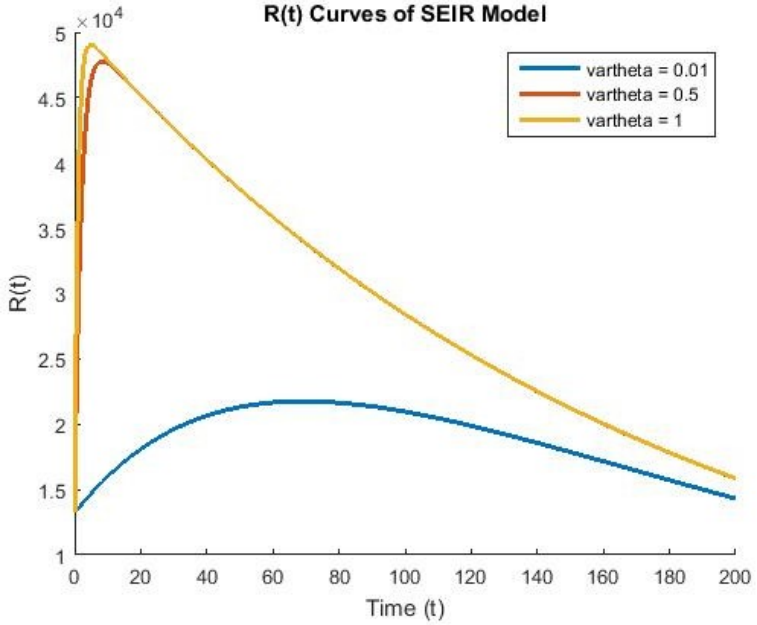

(**a**)

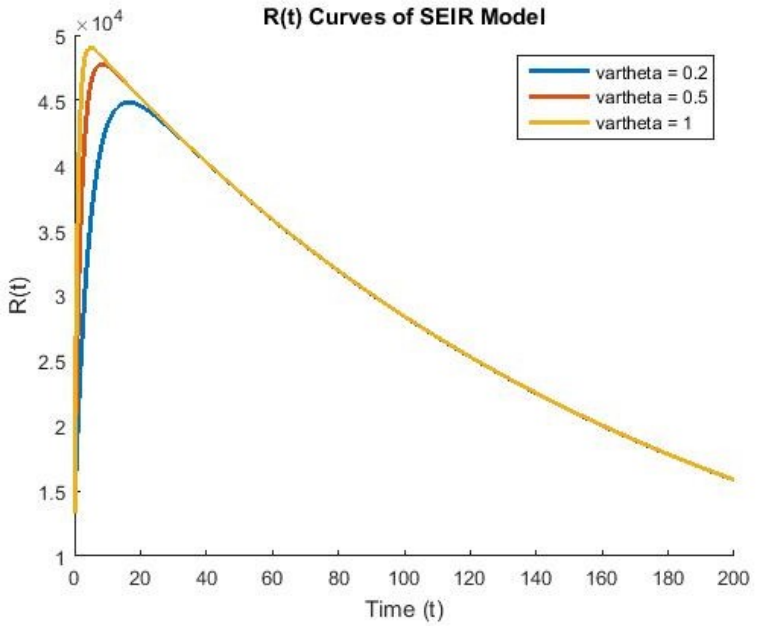

(**b**)

Figure 2. For the recovered people, we have two cases in Figure 2: (**a**) of well-controlled disease with significant recovery numbers at low "ϑ" values. However, in (**b**) it is shown that low "ϑ" values result in strong disease control and a high number of recoveries, while high values lead to greater spread.

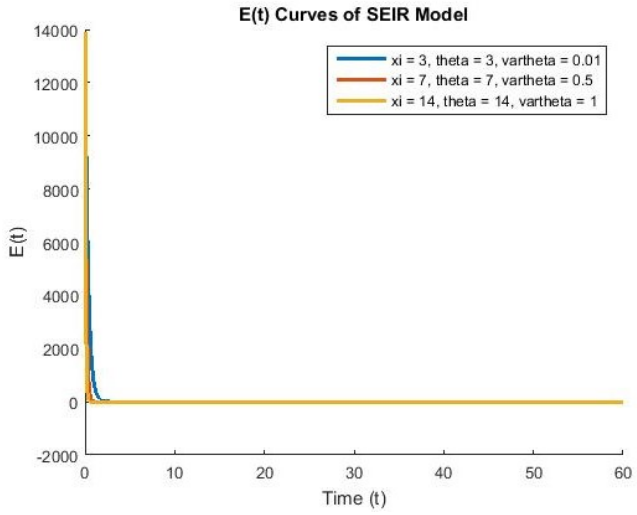

(**a**)

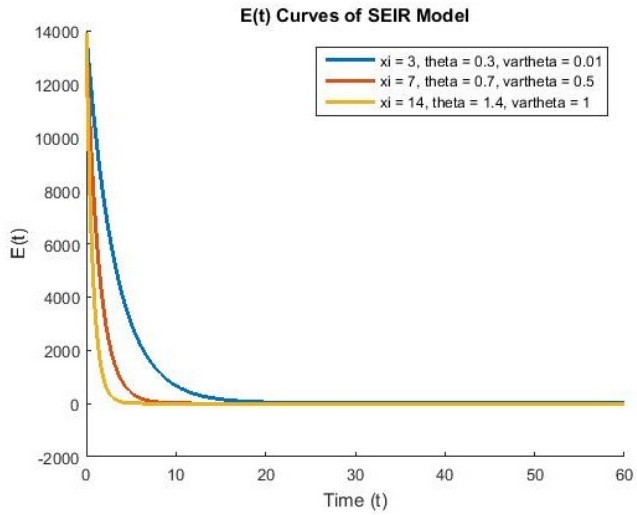

(**b**)

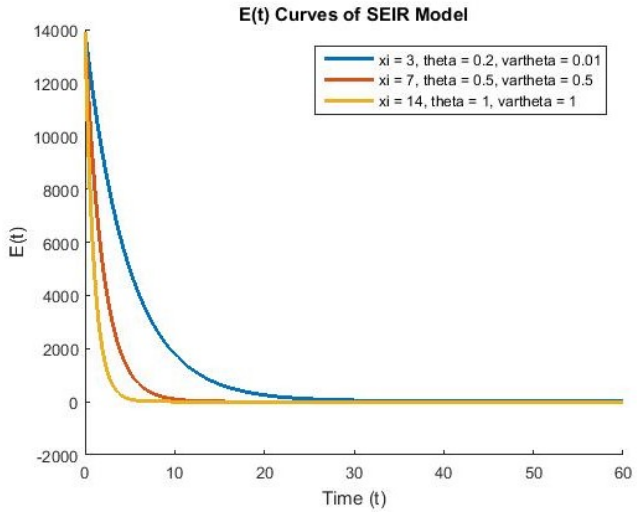

(**c**)

Figure 3. The first graph in Figure 3: (**a**) shows moderate control in an epidemic state. While graph (**b**) shows high disease control effectiveness, indicating a state that is close to free of disease. The best graph (**c**) illustrates a rapid decrease in exposed individuals. In summary, states close to an epidemic in (**a**) and states nearing free of disease in (**b**,**c**) are shown.

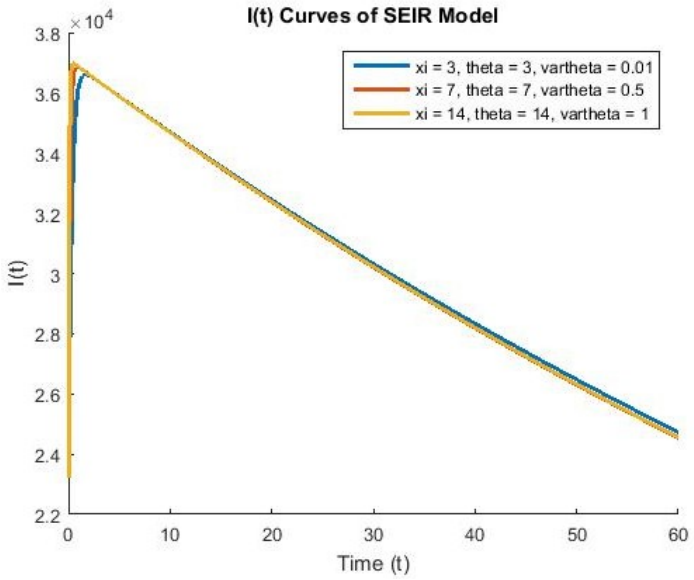

(**a**)

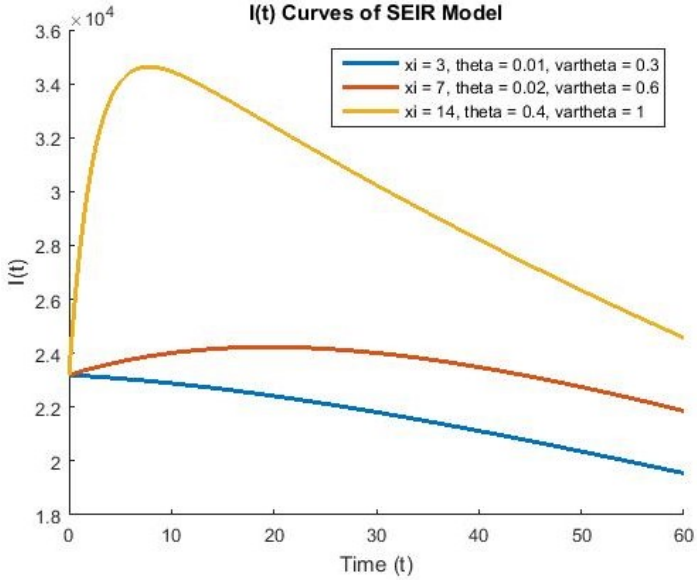

(**b**)

Figure 4. With a consistent decrease from the start, indicating a strong response in Figure 4 the first graph (**b**) exhibits the best control over the disease. Higher ϑ and θ values, on the other hand, may result in moderate-to-poor control of diseases, as in (Figure 3c). This might accelerate the spread of the disease. As a result, the number of infected cases increases more quickly, and control is less effective. All curves gradually decrease but not as successfully as apparent in a graph (**a**), which indicates moderate control. Overall conclusion: a graph (**b**) illustrates the best disease control, whereas the plot (**a**) is in the middle position.

5. Conclusions

We presented a delayed SEIR epidemic model with a latent period for studying local and global stability. We went further into the main role of time delay and how it affected this study. The basic reproductive number, $\Re_0$, is defined and the dynamical behavior of the model is examined. The following is a summary of the study's results. If $\Re_0 < 1$ for all time delays $\xi \geq 0$, then the disease-free equilibrium is locally asymptotically stable. If $\Re_0 > 1$ for all time delays $\xi \geq 0$, then the endemic equilibrium point is locally asymptotically stable. Applying the Lyapunov functional approach and the LaSalle invariance principle, the

endemic equilibrium point is globally asymptotically stable if the reproductive number, $\Re_0$, is greater than unity for all time delays. Hopf bifurcation leads to periodic oscillations and instability for a specific time lag, ξ. An analysis involves the Hopf bifurcation conditions for the endemic equilibrium point. The effect of the time lag parameter, ξ, on the behavior of the infection has been studied. According to the results, the disease can be efficiently controlled and managed by increasing vaccination rates and minimizing interactions through precautionary measures. On the other hand, a higher rate of vaccination and interactions between people may result in moderate-to-poor control of diseases, which might accelerate the spread of the disease. Despite its simplicity, the basic DDE model may control huge population densities and display various dynamics, including quasi-periodic and chaotic patterns. Several other factors affect the speed of disease spread and its control, such as taking precautionary measures and vaccinating young children. We will certainly work on implementing this in future research and will apply it to other diseases like malaria.

Author Contributions: Conceptualization, M.H.H., T.E.-A., G.A., M.A.S. and H.E.-M.; formal analysis, M.H.H., T.E.-A. and M.A.S.; investigation, M.H.H., M.A.S. and G.A.; methodology, M.H.H., T.E.-A., G.A., M.A.S. and H.E.-M.; project administration, M.H.H., H.E.-M. and M.A.S.; resources, M.H.H. and G.A.; software, M.H.H. and T.E.-A.; supervision, H.E.-M., M.A.S. and T.E.-A.; validation, M.H.H., M.A.S. and G.A.; visualization, M.H.H. and M.A.S.; writing—original draft, M.H.H., T.E.-A., M.A.S. and H.E.-M.; writing—review & editing, M.H.H., T.E.-A., G.A., M.A.S. and H.E.-M. All authors have read and agreed to the published version of the manuscript.

Funding: Princess Nourah bint Abdulrahman University Researchers Supporting Project Number (PNURSP2024R45), Princess Nourah bint Abdulrahman University, Riyadh, Saudi Arabia.

Data Availability Statement: The original contributions presented in this study are included in the article. Further inquiries can be directed to the corresponding author.

Conflicts of Interest: The authors declare no conflict of interest.

References

1. Anderson, R.M.; May, R.M. Population Biology of Infectious Diseases: Part I. *Nature* **1979**, *280*, 361–367. [CrossRef] [PubMed]
2. Anderson, R.M.; May, R.M. *Infectious Diseases of Humans: Dynamics and Control*; Oxford University Press: Oxford, UK, 1998.
3. Dieudonné, J. *Foundations of Modern Analysis*; Academic Press: New York, NY, USA, 1960.
4. Capasso, V. *Mathematical Structure of Epidemic Systems, Vol. 97 of Lecture Notes in Biomathematics*; Springer: Berlin, Germany, 1993.
5. Diekmann, O.; Jheesterbeek, J.A.P. *Mathematical Epidemiology of Infectious Disease*; John Wiley & Sons: London, UK, 2000.
6. Hethcote, H.W.; Tudor, D.W. Integral Equation Models for Endemic Infectious Diseases. *J. Math. Biol.* **1980**, *9*, 37–47. [CrossRef] [PubMed]
7. Huo, H.F.; Ma, Z.P. Dynamics of a Delayed Epidemic Model with Non-Monotonic Incidence Rate. *Commun. Nonlinear Sci. Numer. Simul.* **2010**, *15*, 459–468. [CrossRef]
8. McCluskey, C.C. Complete Global Stability for an SIR Epidemic Model with Delay-Distributed or Discrete. *Nonlinear Anal. Real World Appl.* **2010**, *11*, 55–59. [CrossRef]
9. Xiao, D.; Ruan, S. Global Analysis of an Epidemic Model with Non-Monotone Incidence Rate. *Math. Biosci.* **2007**, *208*, 419–429. [CrossRef]
10. Hethcote, H.W.; Stech, H.W.; Vand den Driessche, P. Periodicity and stability in Epidemic Models: A survey. In *Differential Equations and Applications in Ecology, Epidemics, and Population Problems*; Busenberg, S.N., Cooke, K.L., Eds.; Academic Press: New York, NY, USA, 1981; pp. 65–82.
11. Cooke, K.L. Stability Analysis for a Vector Disease Model. *Rocky Mt. J. Math.* **1979**, *9*, 31–42. [CrossRef]
12. Hethcote, H.W.; Van den Driessche, P. An SIS Epidemic Model with Variable Population Size and a Delay. *J. Math. Biol.* **1995**, *34*, 177–194. [CrossRef] [PubMed]
13. Bretta, E.; Hara, T.; Ma, W.; Takeuchi, Y. Global Asymptotic Stability of an SIR Epidemic Model with Distributed Time Delay, Nonlinear Analysis. *Theory Methods Appl. A* **2001**, *47*, 4107–4115. [CrossRef]
14. Song, X.; Cheng, S. A Delay-Differential Equation Model of HIV Infection of CD4T-cells. *J. Korean Math. Soc.* **2005**, *42*, 1071–1086. [CrossRef]
15. Awasthi, A.K.; Kumar, S.; Garov, A.K. A Mathematical Model for Stability Analysis of Covid Like Epidemic/Endemic/Pandemic. *medRxiv* **2021**. [CrossRef]
16. Phitchayapak, W.; Prathom, K. Stability Analysis of SEIR Model Related to Efficiency of Vaccines for COVID-19 Situation. *Heliyon* **2021**, *7*, e06812.

17. Youssef, H.M.; Alghamdi, N.A.; Ezzat, M.A.; El-Bary, A.A.; Shawky, A.M. A Modified SEIR Model Applied to the Data of COVID-19 spread in Saudi Arabia. *AIP Adv.* **2020**, *10*, 125210. [CrossRef] [PubMed]
18. Youssef, H.; Alghamdi, N.; Ezzat, M.A.; El-Bary, A.A.; Shawky, A.M. Study on the SEIQR Model and Applying the Epidemiological Rates of COVID-19 Epidemic Spread in Saudi Arabi. *Infect. Dis. Model.* **2021**, *6*, 678–692. [PubMed]
19. Tipsri, S.; Chinviriyasit, W. Stability Analysis of SEIR Model with Saturated Incidence and Time Delay. *Int. J. Appl. Phys. Math.* **2014**, *4*, 42. [CrossRef]
20. Hassard, B.D.; Azarinoff, N.D.K.; Wan, Y.H. *Theory and Applications of Hopf Bifurcation*; Cambridge University: Cambridge, UK, 1981.
21. Marsden, J.E.; McCracken, M. *The Hopf Bifurcation and Its Applications*; Springer: New York, NY, USA, 1976.
22. Zhang, T.; Liu, J.; Teng, Z. Stability of Hopf bifurcation of a Delayed SIRS Epidemic Model with Stage Structure. *Nonlinear Anal. Real World Appl.* **2010**, *11*, 293–306. [CrossRef]
23. Greenhalgh, D. Effects of heterogeneity on the spread of HIV/AIDS among Intravenous Drug Users in Shooting Galleries. *Math. Biosci.* **1996**, *136*, 141–186. [CrossRef]
24. Greenhalgh, D.; Khan, Q.J.A.; Lewis, F.I. Hopf bifurcation in Two SIRS Density Dependent Epidemic Models. *Math. Comput. Model.* **2004**, *39*, 1261–1283. [CrossRef]
25. Greenhalgh, D.; Khan, Q.J.A.; Lewis, F.I. Recurrent Epidemic Cycles in an Infectious Disease Model with a Time Delay in Loss of Vaccine Immunity. *Nonlinear Anal.* **2005**, *63*, 779–788. [CrossRef]
26. Hethcote, H.W.; Yi, L.; Zhujun, J. Hopf bifurcation in Models for Pertussis Epidemiology. *Math. Comput. Model.* **1999**, *30*, 29–45. [CrossRef]
27. Annas, S.; Paratama, M.I.; Rifandi, M.; Sanusi, W.; Side, S. Stability Analysis and Numerical Simulation of SEIR Model for Pandemic COVID-19 Spread in Indonesia. *Chaos Solitons Fractals* **2020**, *139*, 110072. [CrossRef]
28. Rusliza, A.; Budin, H. Stability Analysis of Mutualism Population Model with Time Delay. *Int. J. Math. Comput. Phys. Electr. Comput. Eng.* **2012**, *6*, 151–155.
29. Diekmann, O.; Heesterbeek, J.A.P.; Roberts, M.G. The Construction of Next-Generation Matrices for Compartmental Epidemic Models. *J. R. Soc. Interface* **2010**, *7*, 873–885. [CrossRef] [PubMed]
30. Anonim 2020. Situasi Kasus Indonesia. Available online: https://covid19.kemkes.go.id/ (accessed on 5 April 2020).
31. Ruan, S.; Wen, J. On the Zeros of Transcendental Functions with Applications to Stability of Delay Differential Equations with Two Delays. *Dyn. Contin. Discret. Impuls. Syst. Ser. A Math. Anal.* **2003**, *10*, 863–874.
32. Willems, J.L. *Stability Theory of Dynamical Systems*; Nelson: New York, NY, USA, 1970.
33. Wei, H.; Li, X.; Martchev, M. An Epidemic Model of a Vector-Borne Disease with Direct Transmission and Time Delay. *J. Math. Anal. Appl.* **2008**, *342*, 895–908. [CrossRef]
34. LaSalle, J.P. *The Stability of Dynamical Systems*; SIAM: Philadelphia, PA, USA, 1976.
35. Hale, J.K.; Lunel, S. *Introduction to Functional Differential Equations*; Springer, New York, NY, USA, 1993.
36. Anonim. Proyeksi Jumlah Penduduk Indonesia 2020. 2020. Available online: https://databoks.katadata.co.id/datapublish/2020/01/02/inilah-proyeksi-jumlah-penduduk-indonesia-2020 (accessed on 29 March 2020).
37. Spencer, J.A.; Shutt, D.P.; Moser, S.K.; Clegg, H.; Wearing, H.J.; Mukundan, H.; Manore, C.A. Epidemiological parameter review and comparative dynamics of influenza, respiratory syncytial virus, rhinovirus, human coronvirus, and adenovirus. *medRxiv* **2020**. [CrossRef]